Low temperature structural anomalies arisen from competing exchange interactions in pyrochlore Nd2Ru2O7 probed by XRD and EXAFS

Journal:	*Physical Chemistry Chemical Physics*
Manuscript ID:	CP-ART-06-2015-003340.R2
Article Type:	Paper
Date Submitted by the Author:	11-Aug-2015
Complete List of Authors:	Chen, Shi-Wei; National Synchrotron Radiation Research Center, Fu, Shao-Wei; National Synchrotron Radiation Research Center, Pao, Chih-Wen; National Synchrotron Radiation Research Center, Lee, Jenn-Min; National Synchrotron Radiation Research Center, Chen, Shin-An; National Synchrotron Radiation Research Center, Haw, Shu-Chih; National Synchrotron Radiation Research Center, Lee, Jyh-Fu; National Synchrotron Radiation Research Center, Liu, Chun-Hsia; National Synchrotron Radiation Research Center, Chang, Chung-Kai; National Synchrotron Radiation Research Center, Chuang, Yu-Chun; National Synchrotron Radiation Research Center, Sheu, Hwo-Shuenn; National Synchrotron Radiation Research Center, Lu, Kueih-Tzu; National Synchrotron Radiation Research Center, Ku, Szu-Tu; National Cheng Kung University, Chang, Lieh-Jeng; National Cheng Kung University, Chen, Jin-Ming; National Synchrotron Radiation Research Center,

PCCP

ARTICLE

Low temperature structural anomalies arisen from competing exchange interactions in pyrochlore $Nd_2Ru_2O_7$ probed by XRD and EXAFS

Received 00th January 20xx,
Accepted 00th January 20xx

DOI: 10.1039/x0xx00000x

www.rsc.org/

Shi-Wei Chen[a], Shao-Wei Fu[a], Chih-Wen Pao[a], Jenn-Min Lee[a], Shin-An Chen[a], Shu-Chih Haw[a], Jyh-Fu Lee[a], Chun-Hsia Liu[a], Chung-Kai Chang[a], Yu-Chun Chuang[a], Hwo-Shuenn Sheu[a], Kueih-Tzu Lu[a], Szu-Tu Ku[b.c], Lieh-Jeng Chang[b,*], and Jin-Ming Chen[a,*]

Quantitative structural parameters of pyrochlore $Nd_2Ru_2O_7$, with temperature dependence, have been derived on fitting XRD and EXAFS data. An anomalous expansion of the lattice parameter and the Ru-O bond length indicate a structural instability at low temperatures; in particular, an increase in the non-thermal term of the mean square fluctuation in the bond length is the evidence for a static disorder of Ru atoms. This static disorder is closely correlated with a decrease in average Ru-O-Ru bond angle with decreasing temperature, favoring the short-range ferromagnetic coupling in the material. This ferromagnetic coupling formed thus triggered the spin frustration at low temperature when the contradictory constraints of antiferromagnetic interaction act upon the same Ru site in the corner-sharing tetrahedrons of pyrochlore $Nd_2Ru_2O_7$. This study demonstrating the spin frustration arisen from the competition of ferromagnetic/antiferromagnetic interactions in pyrochlore $Nd_2Ru_2O_7$ will cause structural instability especially in the atomic scale. That provides a new point of view to help understand its particular magnetic state.

---

[a] National Synchrotron Radiation Research Center, Hsinchu 30076, Taiwan
[b] Department of Physics, National Cheng Kung University, Tainan 70101, Taiwan
[c] Institute of Physics, Academia Sinica, Taipei 11529, Taiwan.
*** E-mail:** jmchen@nsrrc.org.tw (JM Chen); ljchang@mail.ncku.edu.tw (LJ Chang)

Electronic Supplementary Information (ESI) available:

PCCP

ARTICLE

I. Introduction

Pyrochlore oxides with chemical formula $A_2B_2O_7$, in which A is a trivalent rare-earth ion and B is a tetravalent transition-metal ion, have a cubic structure (space group Fd-3m) comprising two interpenetrating B_2O_6 and A_2O' sublattices [1-2]. These materials have attracted considerable attention because, if either A or B are magnetic ions, the magnetic correlations between the ions combined with the geometrical frustration may induce a degeneracy of the magnetic ground states at low temperature. This leads to various intriguing physical phenomena such as a spin-liquid state, in $Tb_2Ti_2O_7$ [3-4], and a spin-ice state, in $Dy_2Ti_2O_7$ [5].

Ruthenium pyrochlores $A_2Ru_2O_7$ (A=Y or rare earth) have been extensively studied in the past decades [6-9]. The partially filled 4*d* shell of Ru^{4+} and the rare-earth magnetic ions form two networks of magnetic corner-sharing tetrahedra. In $A_2Ru_2O_7$, the Ru^{4+} magnetic order occurs in the temperature range of 75 - 160 K depending on the ionic radius of the A^{3+} ion [9-10]. It has been suggested that in $Nd_2Ru_2O_7$ this transition at $T_N \approx 146$ K, which is accompanied by a specific-heat jump and the divergence of the zero-field-cooled (ZFC) and field-cooled (FC) susceptibilities, is due to the Ru moments freezing into an antiferromagnetically coupled state that macroscopically exhibits a spin-glass-like character due to frustration [11]. A second magnetic transition was observed in $Nd_2Ru_2O_7$ as the temperature was reduced below 20 K, and led to a further divergence of the ZFC and FC susceptibilities as well as a hysteresis in the low-temperature field-dependent magnetization [12-13]. Taira *et al.* [13] suggested this was a spin-glass transition, even though a jump in the specific-heat was observed at the corresponding temperature. In contrast, Gaultois *et al.* [2] have asserted that the transition at $T_N \approx 146$ K is to a long-range antiferromagnetically ordered state with a weak ferromagnetism arising from spin canting. The transition at 20 K is not present in their sample. They assign the features seen at 20 K in earlier work to the inclusion of Nd_3RuO_7, a secondary phase that is easily formed during the preparation of $Nd_2Ru_2O_7$. The source of the features in ZFC-FC susceptibilities of $Nd_2Ru_2O_7$ at around 20 K therefore remains uncertain.

As reported, the dominant magnetic interaction in $Nd_2Ru_2O_7$ is antiferromagnetic coupling while there is short-range ferromagnetic coupling existed in the material [2]. The transient ferromagnetic coupling is formed when the contradictory constraints of antiferromagnetic interaction act upon the same Ru site [10]. It infers that the local ferromagnetic coupling formed is crucial to the spin frustration arisen [14]. Furthermore, the spin frustration may accompany structural instability especially in the atomic scale, when the materials have strong spin-lattice coupling, because the competing ferromagnetic/antiferromagnetic superexchange interactions are strongly correlated to bond angle and bond distance between atoms [22]. It is similar to the effect of the spin-driven Jahn-Teller distortion that induces lattice distortions as the two-fold degeneracy of the spin singlets of a tetrahedron led to the spontaneous breakdown of the lattice symmetry [15-16]. However, the precise study on the low temperature atomic environment in pyrochlore $Nd_2Ru_2O_7$ is still rare. Maybe one general belief that thermal motion of atoms should be suppressed at a low temperature, and, to determine the nature and degree of the static disorder is difficult. The lattice disordering in pyrochlores is an important issue because it potentially leads to frustrated interactions, and accordingly spin-glass [17-18] or spin liquid [19] states can arise. We thus intend to explore, in detail, the temperature dependence of the lattice dynamics and especially the atom fluctuation in pyrochlore $Nd_2Ru_2O_7$, figuring out the relation between structural parameters and magnetic interactions. In this study. we focus on $Nd_2Ru_2O_7$ because, in our pre-study, among several of ruthenium pyrochlores such as $Y_2Ru_2O_7$, $Tb_2Ru_2O_7$, $Gd_2Ru_2O_7$, $Ho_2Ru_2O_7$, and $Nd_2Ru_2O_7$, only $Nd_2Ru_2O_7$ shows anomaly in the x-ray diffraction and absorption results at low temperatures. The absorption edges of $Y_2Ru_2O_7$, $Tb_2Ru_2O_7$, $Gd_2Ru_2O_7$, and $Ho_2Ru_2O_7$ remain constant while only that of $Nd_2Ru_2O_7$ shifts to low photon energy with a decreasing temperature. That reflects the increasing bond length of Ru-O in $Nd_2Ru_2O_7$, due to the reducing covalency, at low temperatures and implies the possibility of spin-lattice coupling below T_N.

In this work, the structural variations in the low-temperature phase of $Nd_2Ru_2O_7$ were studied by combining with the high-resolution powder x-ray diffraction (XRD) and extended x-ray absorption fine structure (EXAFS) techniques. XRD technique explored the structural instability of $Nd_2Ru_2O_7$ at low temperatures while EXAFS technique, with a powerful ability to detect local environment of atoms, allowed us to study the structure on an atomic scale so that the static-disorder lattice of $Nd_2Ru_2O_7$ at low temperature can be determined. With accompanying magnetic measurements, the importance of the lattice degrees of freedom on the peculiar magnetic state is clearly manifested.

II. Experimental details

Polycrystalline $Nd_2Ru_2O_7$ was synthesized from pure materials Nd_2O_3 (99.99 %) and RuO_2 (99.9 %) mixed in stoichiometric proportions. The powders were pelletized with an iso-static cold press and heated in air at 1073 K for 12 hours, and then reacted at 1423 K over four days with several intermediate grindings. Powder x-ray diffraction showed that the resulting samples to have formed with a cubic structure and a lattice parameter of 10.354 Å at room temperature. No impurity phases were detected in the diffraction patterns of the powders to within an accuracy of a few percent

Dc magnetization measurements versus temperatures were made using a commercial superconducting quantum interference device (SQUID) magnetometer (Quantum Design MPMS system). A small magnetic field of 100 Oe was applied in the measurements.

X-ray diffraction measurements as a function of temperatures were carried out using the beamline BL01C2 of the National Synchrotron Radiation Research Center (NSRRC) in Taiwan. The incident x-rays (wavelength 0.62 Å, 20 keV) were generated from a superconducting wavelength-shifter source and a Si (111) double-crystal monochromator. $Nd_2Ru_2O_7$ powders were injected into a glass capillary and mounted on an aluminum carrier. X-ray diffraction patterns were collected with an imaging plate area detector (Mar345) at different temperatures down to 10 K. Fit2D software was used to extract XRD data; the GSAS package was used to refine the raw data using the Rietveld method, to derive structural parameters.

Ru *K*-edge x-ray absorption spectra (x-ray absorption near edge structure, XANES, and extend x-ray absorption fine structure, EXAFS) at low temperature were recorded in situ at beamline BL01C2, in NSRRC, Taiwan. A fixed-exit double-crystal Si(111) monochromator served to tune the x-ray photon energy controlling an average energy resolution $\Delta E/E$ = 1.6 x 10^{-4}. The monochromatized beam was then focused with a bent toroidal refocusing mirror. A Lytle detector was used to collect fluorescence emitted from the powder sample. For energy calibration, a reference compound RuO_2 was measured with an ionization chamber. A standard procedure of data reduction was used to extract the EXAFS functions from the raw experimental data. To compensate for the abruptly decreased amplitude at high energy, the obtained χ functions were decorated with a weighting factor k^3. k^3-weighted $\chi(k)$ data in the *k*-space in ranges 2.9 - 11.5 Å^{-1} for the Ru *K* edge were thus subjected to Fourier transformation to *r*-space to distinguish the EXAFS contributions from the other coordination shells. EXAFS in the *r*-space from 1.8 to 3.2 Å were fitted using theoretical phase and amplitude functions with the IFEFFIT package. Fits were made in an initial series on the Ru *K*-edge k^3-weighted data on fixing the coordination numbers of O, Ru and Nd atoms at 4.74, 5.81 and 5.81, respectively. Local structural parameters were thus quantitatively extracted from the FT$|k^3\chi(R)|$ functions.

III. Results and discussions

Figure 1 shows the dc susceptibility of pyrochlore $Nd_2Ru_2O_7$ measured in the temperature range 2 - 180 K. A difference between ZFC and FC curves starts at 146 K, on cooling, this difference increases further as the temperature reducing below 21 K. According to some reports [2,8], the ZFC-FC difference of the magnetic susceptibility of $Nd_2Ru_2O_7$ at 146 K can be attributed to the antiferromagnetic ordering of Ru^{4+} 4*d* spins with a macroscopically spin-glass-like character due to the frustration. As shown in Figure 2, the dominant antiferromagnetic interaction in $Nd_2Ru_2O_7$ can be indicated by a negative Weiss temperature (θ_{cw}), determined from a fit to high temperature susceptibility data, whereas a deviation from an ideal Curie-Weiss behavior at lower temperature suggests the presence of short-range ferromagnetic correlations. The competition between antiferromagnetic and ferromagnetic interactions is invoked to account for the spin frustration. Due to the arisen spin frustration at low temperatures, the ZFC-FC divergence of the magnetic susceptibility of pyrochlore $Nd_2Ru_2O_7$ further enlarges and cusps appear in the magnetic susceptibility as the temperature down to 21 K. These characteristics at 21 K were also observed in reports [2, 13], in which, Taira *et al.* [13] assigned the characteristics to a spin-glass transition while Gaultois *et al.* [2] asserted the features arisen from the inclusion of Nd_3RuO_7. However, in this study, while there is a difference in the ZFC-FC dc magnetic susceptibility at 21 K there is no feature at this temperature in the specific-heat measurement of our sample of $Nd_2Ru_2O_7$ [20] and the inclusion of Nd_3RuO_7 is excluded through synchrotron x-ray analyses. We thus propose that the increased ZFC-FC difference of the magnetic susceptibility of pyrochlore $Nd_2Ru_2O_7$ at 21 K is due to a further canting of the enhanced ferromagnetic component first seen at 146 K. This variation is accompanied by changes in the structure, the details of which, are discussed later.

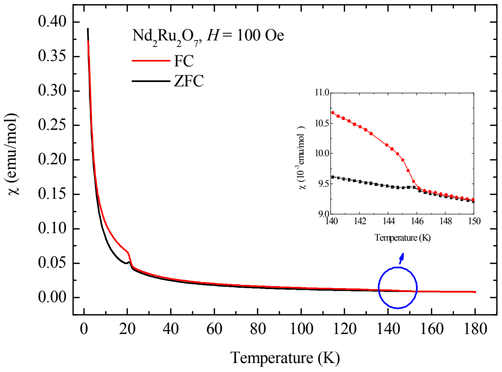

FIG. 1. (color online) DC susceptibility χ measured as a function of temperature for pyrochlore $Nd_2Ru_2O_7$.

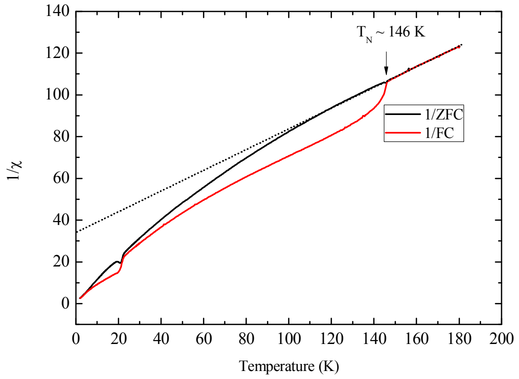

FIG. 2. (color online) inverse susceptibility as a function of temperature for pyrochlore $Nd_2Ru_2O_7$.

To explore in detail the structural variations of pyrochlore $Nd_2Ru_2O_7$, as a function of temperature, and to deduce the relative influences on the magnetic properties, we recorded x-ray absorption and diffraction patterns in situ at low temperature with the synchrotron x-ray source. X-ray diffraction patterns provide information on the lattice structure while x-ray absorption is a powerful technique to probe the orbital and atomic structures of materials.

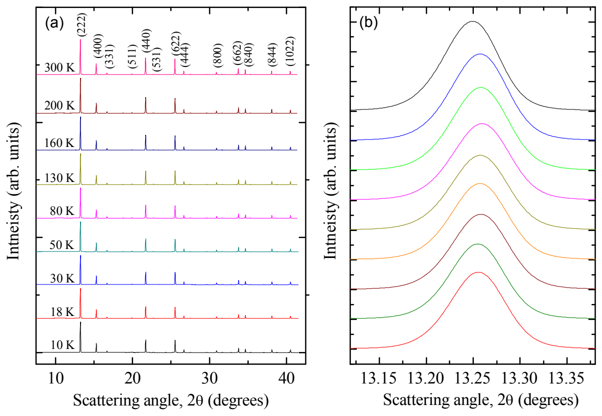

Fig. 3 (color online) (a) Representative x-ray diffraction patterns of $Nd_2Ru_2O_7$ collected in situ at various temperatures. (b) Enlargement of the main peaks in x-ray diffraction patterns of $Nd_2Ru_2O_7$. (c) X-ray diffraction patterns of $Nd_2Ru_2O_7$ collected at 10 K, with the corresponding Rietveld refinements (red line) and residuals (blue line). The rows of the vertical marks correspond to the calculated peak positions of $Nd_2Ru_2O_7$.

Figure 3(a) displays the representative x-ray diffraction patterns of pyrochlore $Nd_2Ru_2O_7$ taken in situ at temperatures from 295 to 10 K; these patterns show the material has a cubic structure with space group Fd-3m. No additional diffraction peaks or phase transformations were observed for temperatures down to 10 K; the variations of the relative peak intensities and positions, Figure 3(b), mainly reflect an altered atomic distribution and lattice parameters. To investigate in detail the structural variations of pyrochlore $Nd_2Ru_2O_7$ with temperatures, we refined the XRD data using the Rietveld method. Rietveld analysis of the powder diffraction patterns enabled us to determine the crystal structure giving the lattice parameters and atomic positions. These structural parameters for $Nd_2Ru_2O_7$ deduced from the diffraction data at selected temperatures are presented in Table I. Satisfactory agreement between the experimental data and the Rietveld refinements is evident from the small values of reliability parameters R_{wp}, R_p, and χ^2 shown in Table I.

Table I Structural parameters of pyrochlore $Nd_2Ru_2O_7$ at selected temperatures, refined using the Rietveld method.

T /K	300	200	160	130	100	50	10
lattice parameter							
a /Å	10.3544 (5x10⁻⁴)	10.3440 (3X10⁻⁴)	10.3412 (2x10⁻⁴)	10.3420 (4x10⁻⁴)	10.3394 (3x10⁻⁴)	10.3373 (2x10⁻⁴)	10.3388 (3x10⁻⁴)
Ru-Ru/Å	3.6608 (4.2x10⁻⁴)	3.6596 (2X10⁻⁴)	3.6582 (1x10⁻⁴)	3.6555 (4.1x10⁻⁴)	3.6558 (2x10⁻⁴)	3.6556 (1x10⁻⁴)	3.6553 (3x10⁻⁴)
Ru-Nd/Å	3.6608 (9x10⁻⁴)	3.6596 (7X10⁻⁴)	3.6582 (1x10⁻⁴)	3.6555 (9x10⁻⁴)	3.6558 (6x10⁻⁴)	3.6556 (3x10⁻⁴)	3.6553 (8x10⁻⁴)
atomic positions							
Nd	0.5000 (0)	0.5000 (0)	0.5000 (0)	0.5000 (0)	0.5000 (0)	0.5000 (0)	0.5000 (0)
Ru	0.0000 (0)	0.0000 (0)	0.0000 (0)	0.0000 (0)	0.0000 (0)	0.0000 (0)	0.0000 (0)
O1	0.3309 (5x10⁻⁴)	0.3310 (1x10⁻⁴)	0.3312 (3x10⁻⁴)	0.3314 (5x10⁻⁴)	0.3315 (5x10⁻⁴)	0.3317 (3x10⁻⁴)	0.3319 (5x10⁻⁴)
O2	0.3750 (0)	0.3750 (0)	0.3750 (0)	0.3750 (0)	0.3750 (0)	0.3750 (0)	0.3750 (0)
reliability Factors							
R_p /%	3.99	3.88	3.94	4.08	4.22	4.12	3.90
R_{wp} /%	5.70	5.61	5.78	5.75	5.66	5.56	5.57
χ^2	1.12	0.72	0.82	1.08	0.97	0.69	1.09

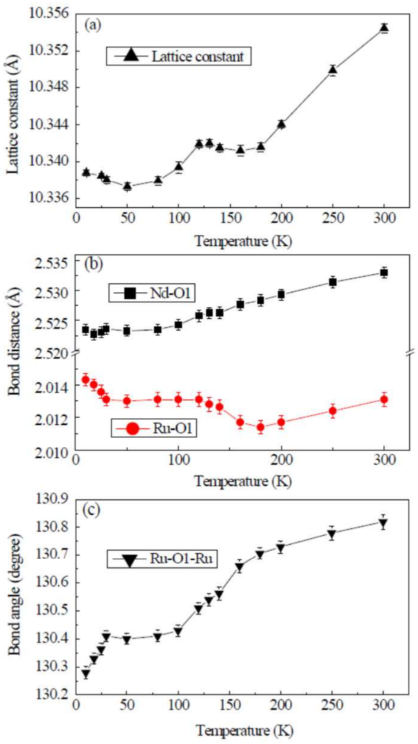

FIG. 4. (color online)Temperature dependence of (a), the lattice parameter, (b) Nd-O and Ru-O distance, and (c) Ru-O-Ru bond angle of pyrochlore $Nd_2Ru_2O_7$.

To elucidate the variations in the structure, we reproduce the temperature dependence of the lattice parameter, the Nd-O distance, the Ru-O distance, and the Ru-O-Ru bond angle as shown in Figure 4(a) - 4(c), respectively. All these values are calculated from the structural parameters determined via the XRD refinement. As noted in Figure 4(a), the $Nd_2Ru_2O_7$ lattice parameter initially displays a typical thermal contraction with decreasing temperature, but then increases slightly below 160 K with a maximum in the temperature range 130 - 120 K, and eventually undergoes an anomalous expansion below 50 K. Ru-Ru bond distance shows a similar trend. As shown in Figure 4(b) and 4(c), the Ru-O bond length, rather than the Nd-O bond length, also increases around 160 K and the Ru-O-Ru bond angle decreases in the same temperature range. These results indicate a structural instability, such as lattice distortion, of $Nd_2Ru_2O_7$ and intriguing behavior is actually happening at the Ru site. That is quite unique in contrast with a typical reduction in bond length and recovery of lattice symmetry, ascribed to shrinkage, observed in most materials as the temperature is reduced [21]. The temperatures at which these anomalies occur are close to those of magnetic transitions in the dc susceptibility as shown in Figure 1. The importance of spin-lattice coupling in pyrochlore $Nd_2Ru_2O_7$ is thus strongly implied. Kanamori-Goodenough rule introduces a large metal-O-metal bond angle favorite antiferromagnetic coupling whereas a small metal-O-metal bond angle trending to cause ferromagnetic coupling [22-23]. Shimakawa *et al.* [24] have also applied this rule to explain the ferromagnetic behavior associated with a superexchange interaction of Mn^{4+} spins at an intermediate

Mn-O-Mn bond angle of about 130° in the Mn pyrochlore. The sharply reduced bond angle of Ru-O-Ru in pyrochlore $Nd_2Ru_2O_7$ in specific temperature ranges may therefore also be related to the favoring of ferromagnetic interactions. This is consistent with the data, shown in Figure 2, presenting the co-existence of short-range ferromagnetic correlations with the dominant antiferromagnetic interactions. In references, the weak ferromagnetic component, associated with the antiferromagnetic ordering of Ru^{4+} 4*d* spins [2] as the temperature is reduced below 146 K, and the ferromagnetic hysteresis, at 5 K [12], have already been observed in pyrochlore $Nd_2Ru_2O_7$.

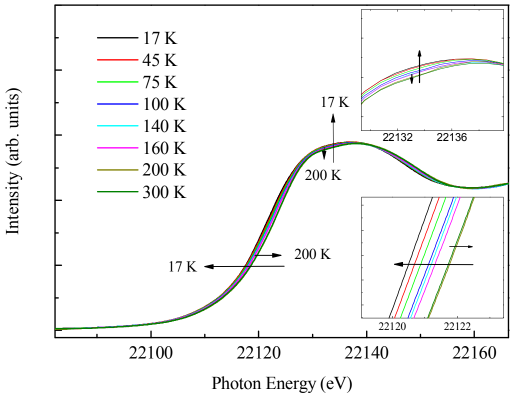

FIG. 5. (color online) Ru *K*-edge XANES spectra of $Nd_2Ru_2O_7$ recorded at various temperatures.

We also investigated the evolution of the local atomic environment with temperature in $Nd_2Ru_2O_7$ by probing in-situ Ru *K*-edge x-ray absorption spectra. In the XANES region of the spectra, the absorption edge and peak intensity reflect the valence and unoccupied density of states of the absorbing atoms, respectively, whereas, in the EXAFS region, multiple scattering provides information about the local atomic environment [25]. Figure 5 displays Ru *K*-edge XANES spectra of pyrochlore $Nd_2Ru_2O_7$ at different temperatures. An enlargement of the absorption edge is shown in the inset. As indicated by the arrow, the absorption edge shifts to higher energy as the temperature reduced to 200 K, reflecting the raised covalency between Ru and O atoms, as well as the shrink of Ru-O bond. While the edges opposite shift to lower energy when the temperature continuously decreases below 200K. This shift indeed reflects the weakened covalency between Ru and O atoms. That could attribute to an elongation of Ru-O bond or an alteration in the symmetry of Ru-O tetrahedral, resulting in the reduced overlap between Ru and O orbitals. This trend is consistent with the results obtained by fitting XRD data. As shown in Figure 4 (b), Ru-O bond distance decreases initially and increases with the decreasing temperature. In Figure 5, the main peaks of Ru K-edge absorption spectra get higher as the temperature decreasing below 200K. Because Ru K-edge absorption refers to 1*s* - 4*p* electron transition. The higher intensity of the main peak, at a low temperature, thus manifests the higher Ru 4*p* un-occupied density of states. Accordingly, a weakened covalency between Ru and O atoms at a low temperature is expected. This result coincides with the discussion above.

We have also probed Ru L_3-edge spectra of $Nd_2Ru_2O_7$ in this study, see supplemental material [20]. The spectra keep constant when the temperature decreasing to 8K. Ru L_3-edge spectra refer to electron transition from 2*p* to 4*d*. The constant intensity of the main peak thus reflects the uniformity of Ru 4*d* density of states. Accordingly, one can realize that the reduced covalency of $Nd_2Ru_2O_7$ at a low temperature associated with Ru 4*p* and O 2*p* orbitals but not Ru 4*d* and O 2*p* orbitals.

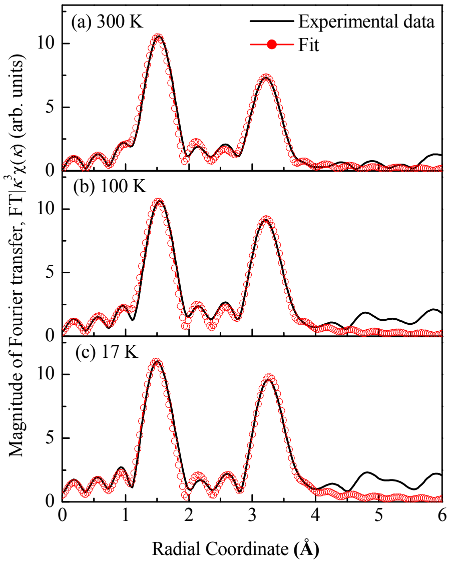

FIG. 6. (color online) k^3-weighted Fourier-transformed EXAFS functions at the Ru *K*-edge of pyrochlore $Nd_2Ru_2O_7$ at (a) 300 K, (b)100 K, and (c) 17 K, with their corresponding fits.

EXAFS oscillations occurring above a core-level x-ray absorption edge result from an interaction between an outgoing photoelectron, from the absorbing atom, and the photoelectron backscattered by neighboring atoms. The oscillations are periodic in pair distance *r* and photoelectron wave number $k = \sqrt{2m(E - Eo)/\hbar}$ in which *E* is the incident x-ray energy and E_0 is the energy at the absorption edge. EXAFS analysis yields information about the radial distribution of distance around the absorbing atoms. In particular, the pair distances r_i and the mean square of the fluctuation in the interatomic distance (bond length), σ_i^2 , can be obtained for the first few atomic shells; σ_i^2 includes a dynamic term due to the thermal motion of the atoms and a static term due to the structural disorder. Figure 6(a) - 6(c) display the k^3-weighted Fourier-transformed EXAFS functions (FT| $k^3\chi(R)$) at the Ru *K* edge of pyrochlore $Nd_2Ru_2O_7$ at 300, 100 and 17 K, respectively, with their corresponding fits. The data display two pronounced features at 1.5 and 3.2 Å in the radial coordinate reflecting the bond lengths between the Ru atom and the atoms in the first and second shells, respectively. The former corresponds to the

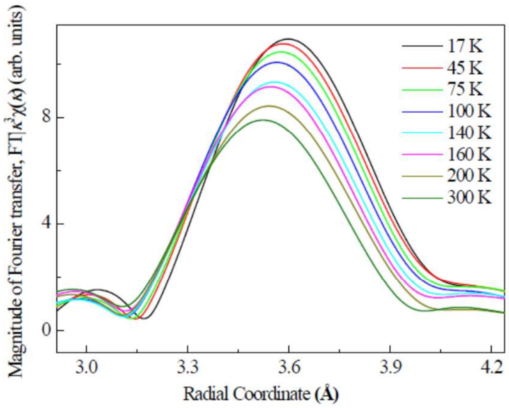

FIG. 7. (color online) Integration of the Fourier-transformed EXAFS data of $Nd_2Ru_2O_7$ at various temperatures.

Ru-O bond length and the latter to the Ru-M (M = Ru or Nd) distance. Figure 7 shows an integration of the Fourier-transformed EXAFS data of pyrochlore $Nd_2Ru_2O_7$ at various temperatures from 300 to 17 K focusing on only the second-shell radial coordinate (Ru-Ru or Ru-Nd). The magnitude of the Fourier transform increased and the corresponding width broadened with decreasing temperature, which indicates a variation of, for instance, the radial coordination and structural ordering; detailed fits are necessary to obtain quantitative information. Using the IFEFFIT package, we fit the $\chi(k)$ data to the theoretical calculations of FEFF. The satisfactory agreement between the Fourier- transformed data and the fitted curves, as displayed in Figure 6, verifies the accuracy of the fits. Figure 8 shows the temperature dependence of the mean square fluctuation of the bond length, σ^2_{total}, extracted from the functions in an improved curve-fitting procedure [26]. As indicated, with decreasing temperature below 150 K, the mean square fluctuation in the bond length of the Ru-Nd pair decreased monotonically, whereas that of the Ru-O couple, remained nearly constant and that of the Ru-Ru pair, slightly increased. Actually, especially noteworthy is the rigid characteristics of mean square fluctuations of both Ru-O and Ru-Ru. Because the mean square fluctuation of the bond length ($\sigma^2_{\text{total}} = \sigma^2_{\text{static}} + \sigma^2_{\text{thermal}}$) contains a thermal term, $\sigma^2_{\text{thermal}}$, and non-thermal term, σ^2_{static}. $\sigma^2_{\text{thermal}}$ must reduce with decreasing temperature. On that situation, any raised, or even constant, value of σ^2_{total} at low temperatures will indicate the raised σ^2_{static}. Therefore, the nearly constant σ^2_{total} of Ru-O pair and slightly increased σ^2_{total} value of Ru-Ru pair at low temperatures really reflect raised value of σ^2_{static}, as well as the static disorder of Ru site in pyrochlore $Nd_2Ru_2O_7$.

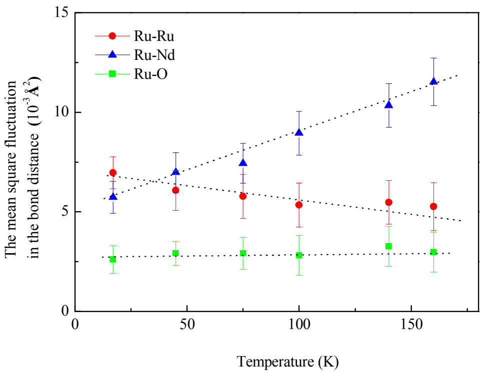

FIG. 8. (color online) Temperature dependence of the mean square fluctuations in bond distances of Ru-Ru, Ru-Nd, and Ru-O pairs.

In pyrochlores, geometrical frustration is an important characteristic that induces a degeneracy of the magnetic ground states and leads to various intriguing physical phenomena at low temperatures [10]. Spin frustration can occur as illustrated in Figure 9. Under the constraint of antiferromagnetic coupling in the nearest neighbor ions, frustration results when contradictory constraints act upon the same site in a material. This situation gets much more complex in tetrahedral [10]. In the case of pyrochlore $Nd_2Ru_2O_7$, spin frustration arises from the presence of short-range ferromagnetic correlations, co-existed with the dominant antiferromagnetic couplings [2, 8]. One possibility of spin frustration is expected to occur on the network of magnetic corner-sharing tetrahedrons constructed by Ru^{4+} ions alone [$\bar{1}10$] direction in the $Fd\bar{3}m$ structure of pyrochlore $Nd_2Ru_2O_7$. The behavior is illustrated in Figure 10. A transient ferromagnetic coupling locally formed at a low temperature accompanies with the reduced Ru-Ru bond distance, Ru-O-Ru bond angle, and increased Ru-O bond distance. The static disorder of Ru sites at low temperatures also arises as frustration. This mode conforms to Kanamori-Goodenough rule, in which, covalent mixing between metal and oxygen atoms drives antiferromagnetic coupling upon a large metal-O-metal bond angle (a 180º superexchange), whereas a small metal-O-metal bond angle (a 90º superexchange) leads to ferromagnetic interaction mediated by delocalized or weakly localized 3d holes [22-23]. The weakened covalence between Ru and O atoms in $Nd_2Ru_2O_7$ at low temperatures, deduced by Ru *K*-edge spectra, may thus decline the antiferromagnetic coupling. Ferromagnetic interaction thus arises with the decreasing Ru-O-Ru bond angle (Figure 4(c)), and rising Ru 4*p* unoccupied density of state (Figure 5).

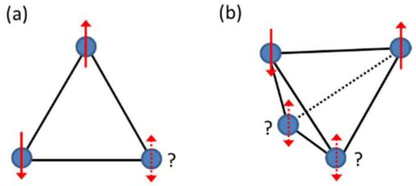

FIG. 9. (color online) Illustration of spin frustration in (a) triangle, and (b) tetrahedron.

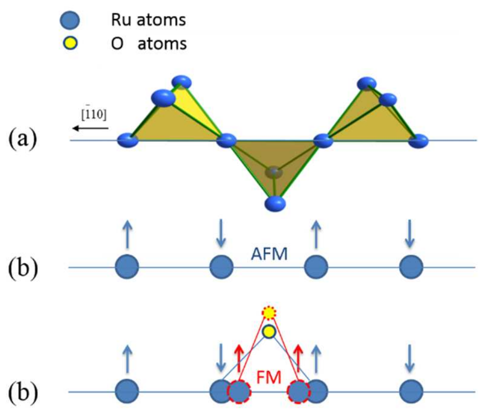

FIG. 10. (color online)(a) The network of magnetic corner-sharing tetrahedrons constructed alone [$\bar{1}10$] direction in the structure of pyrochlore $Nd_2Ru_2O_7$. (b) illustrates the antiferromagnetic ordering, while (c) illustrates the formation of transient ferromagnetic coupling when two Ru atoms approach and Ru-O-Ru bond angle reduces.

IV. Conclusions

This study demonstrates the dominant magnetic interaction in $Nd_2Ru_2O_7$ is antiferromagnetic coupling while there is short-range ferromagnetic coupling enhanced at low temperature in the material. A transient ferromagnetic coupling locally formed at low temperature, due to spin frustration, will cause structural instability. An anomalous expansion of the lattice parameter and Ru-O bond length as well as a reduced Ru-O-Ru bond angle in $Nd_2Ru_2O_7$ upon decreasing temperature below ~ 150 K are thus observed, consistent with the spin frustration occurred at T_N=146 K and the arisen one at 21 K. Static Ru disorder at low temperatures is also realized through a non-thermal term of the mean square fluctuation of the bond length deduced from EXAFS data. That especially evidences the atom position fluctuation are strongly correlated to spin frustration. In this work, we demonstrate the strong dependence between spin and lattice degrees of freedom in pyrochlore $Nd_2Ru_2O_7$. That is crucial to realize comprehensively its exotic magnetic characteristics.

Acknowledgments

National Synchrotron Radiation Research Center and the Ministry of Science and Technology of Taiwan the Republic of China (grant Nos. MOST 102-2113-M-213-004-MY3, and MOST 101-2112-M-006-010-MY3 provided support.

References

[1] M. A. Subramanian, G. Aravamudan, and G. V. Subba Rao, Prog. Solid State Chem. 1983, **15**, 55.
[2] M. W. Gaultois, P. T. Barton, C. S. Birkel, L. M. Misch, E. E. Rodriguez, G. D. Stucky, and R. Seshadri, J. Phys.: Condens. Matter 2013, **25**, 186004.
[3] M. J. P. Gingras, B. C. den Hertog, M. Faucher, J. S. Gardner, S. R. Dunsiger, L. J. Chang, B. D. Gaulin, N. P. Raju, and J. E. Greedan, Phys. Rev. B 2000, **62**, 6496.
[4] H. Takatsu, H. Kadowaki, T. J. Sato, J. W. Lynn, Y. Tabata, T. Yamazaki, and K. Matsuhira, J. Phys.: Condens. Matter 2012, **24**, 052201.
[5] A. P. Ramirez, A. Hayashi, R. J. Cava, R. Siddharthan, and B. S. Shastry, Nature 1999, **399**, 333.
[6] M. Miyazaki, R. Kadono, K. H. Satoh, M. Hiraishi, S. Takeshita, A. Koda, A. Yamamoto, and H. Takagi, Phys. Rev. B 2010, **82**, 094413.
[7] J. Park, K. H. Kim, H. J. Noh, and S.-J. Oh, Phys. Rev. B 2004, **69**, 165120.
[8] M. Ito, Y. Yasui, M. Kanada, H. Harashina, S. Yoshii, K. Murata, M. Sato, H. Okumura, and K. Kakurai, J. Phys. Soc. Jpn. 2000, **69**, 888.
[9] M. Ito, Y. Yasui, M. Kanada, H. Harashina, S. Yoshii, K. Murata, M. Sato, H. Okumura, K. Kakurai, J. Phys. Chem. Solids 2001, **62**, 337.
[10] J. S. Gardner, M. J. P. Gingras, and J. E. Greedan, Rev. Mod. Phys. 2010, **82**, 53.
[11] L. J. Chang, M. Prager, J. Perßon, J. Walter, E. Jansen, Y. Y. Chen, and J. S. Gardner, J. Phys.: Condens. Matter 2010, **22**, 076003.
[12] N. Taira, M. Wakeshima, and Y. Hinatsu, J. Phys.: Condens. Matter 1999, **11**, 6983.
[13] N. Taira, M. Wakeshima, and Y. Hinatsu, J. Solid State Chem. 2000,**152**, 441.
[14] S. T. Bramwell, and M. J. Harris, J. Phys.: Condens. Matter 1998, **10**, L215.
[15] H. Meskine, H. König, and S. Satpathy, Phys. Rev. B 2001, **64**, 094433.
[16] O. Tchernyshyov, R. Moessner, and S. L. Sondhi, Phys. Rev. B 2002, **66**, 064403.
[17] A. P. Ramirez, Annu. Rev. Mater. Sci. 1994, **24**, 453.
[18] C. H. Booth, J. S. Gardner, G. H. Kwei, R. H. Heffner, F. Bridges, and M. A. Subramanian, Phys. Rev. B 2000, **62**, R755.
[19] J. P. C. Ruff, B. D. Gaulin, J. P. Castellan, K. C. Rule, J. P. Clancy, J. Rodriguez, and H. A. Dabkowska, Phys. Rev. Lett. 2007, **99**, 237202.
[20] See Supplemental Material at [*URL will be inserted by publisher*] for the temperature dependence of specific heat capacity and Ru *L*-edge XANES spectra of $Nd_2Ru_2O_7$.
[21] T. K. Wallace, R. H. Colman, and A. C. Mclaughlin, Phys.Chem. Chem. Phys. 2013, **15**, 8672.
[22] J. Kanamori, J. Phys. Chem. Solids 1959, **10**, 87.
[23] J. B. Goodenough, (1963). Magnetism and the Chemical Bond. Interscience-Wiley, New York.
[24] Y. Shimakawa, Y. Kubo, N. Hamada, J. D. Jorgensen, Z. Hu, S. Short, M. Nohara, and H. Takagi, Phys. Rev. B 59, 1249 (1999).
[25] E. Giangrisostomi, M. Minicucci, A. Trapananti, and A. D. Cicco, Phys. Rev. B 2011, **84**, 214202.
[26] Y. L. Soo, Z. H. Ming, S. W. Huang, Y. H. Kao, R. N. Bhargava, and D. Gallagher, Phys. Rev. B 1994, **50**, 7602.